JTTEE5 7:58-63

In-Flight Particle Measurements of Twin Wire Electric Arc Sprayed Aluminum

D.L. Hale, W.D. Swank, and D.C. Haggard

(Submitted 3 August 1997; in revised form 17 October 1997)

A real-time, nonintrusive measurement technique was successfully applied to a Tafa Model 9000 (TAFA Incorporated, Concord, NH) twin wire electric arc thermal spray system to simultaneously measure particle size, velocity, and temperature within the spray plume. Aluminum wire was sprayed with the current varied from 100 to 300 amp, and the gun pressure (air flowrate) varied from 40 to 75 psia. For all cases, the average sizes of the molten aluminum particles along the spray centerline range from 33 to 53 μm. The particles accelerate to peak velocities between 130 and 190 m/s, then decelerate slightly as they travel downstream. The average centerline particle temperature ranges from 2004 to 2056 °C, and the temperature profile remains fairly flat throughout transport to the substrate. A stagnation pressure probe was used to quantify the gas flow regime in the unladen jet. The wires were found to have a pronounced effect on the flow, resulting in a complex three-dimensional flowfield with mixed regions of subsonic and supersonic flow.

Keywords aluminum atomization, inflight particle diagnostics, inflight particle pyrometry, laser Doppler velocimeter, twin-wire electric arc

1. Introduction

The purpose of these experiments was to gain an understanding of the physics of the particle-laden spray flowfield produced by a twin-wire electric arc (TWEA) spray system. The design of this system consists of two electrically insulated wires brought together downstream of an orifice. An electric arc is struck between the wires, causing the wire tips to melt. A high speed gas, in this case air, flows past the wires, stripping off molten droplets and atomizing them. The air flow transports the molten droplets to a substrate where the successive accumulation of droplet splats forms a coating.

The experiments were performed in the thermal spray laboratory at the Idaho National Engineering and Environmental Laboratory using a measurement technique originally designed for use with plasma spray guns (Ref 1-2). An Aerometrics, Inc. (Sunnyvale, CA) Doppler signal analyzer (DSA) Model 3120 laser Doppler velocimeter (LDV) was used to measure particle size and velocity (Ref 3), and an In-Flight Particle Pyrometer (IPP) Model 2000 (TAFA Incorporated, Concord, NH) was used to measure particle temperature.

2. Measurement Technique

A phase Doppler anemometer was used to measure the particle velocity, size, and relative number density within the flow. The phase Doppler method is based on the principles of light scattering interferometry. Measurements are made at a small, nonintrusive optical probe volume defined by the intersection of two argon ion laser beams. The measurement volume is oval, or football-shaped, and approximately 200 μm^3. As a particle passes through the probe volume, it scatters light from the beams and creates an interference fringe pattern.

A receiving lens is located at an off-axis collection angle of 30° and projects this fringe pattern onto 3 detectors. Each detector produces a Doppler burst signal with a frequency proportional to an individual particle velocity. The phase shift between the Doppler burst signals from different detectors is proportional to the size of the particle. All optics and the laser are rigidly mounted on a precision three-axis translatable table. The position of the table is computer controlled, resulting in a precise movement of the measurement volume relative to the spray gun. An argon ion laser operating in the green at 514 nm is used for the LDV. Particle sizing with the phase Doppler method requires the measurement of the phase shift between pairs of Doppler burst signals generated by individual particles (Ref 1).

The velocity and size of 1000 particles is measured at a single location and then arithmetically averaged. The processing algorithm assumes the particles to be smooth spheres. The count rate gives a measure of the relative number density. The phase Doppler method requires no calibration because the particle size and velocity are dependent only on the laser wavelength and optical configuration. Uncertainty in the size and velocity measurement is estimated at ±5%. Further details of the size and velocity measurement technique are available in the literature (Ref 4-6).

Particle temperature is measured with a two-color pyrometric technique. The ratio of light intensity emitted from the hot particle at two different wavelengths is proportional to the temperature of the particles. The measurement volume is pencil shaped, 5 mm in diameter, and approximately 50 mm long. This measurement volume is projected coincidental with that of the size and velocity measurements. The temperature read by the IPP is an average of all particles in this volume, heavily weighted toward the high number density of the spray. For most applications, this is the portion of the spray which forms the

D.L. Hale, W.D. Swank, and **D.C. Haggard,** Lockheed Martin Idaho Technologies Company, Idaho National Engineering and Environmental Laboratory, P.O. Box 1625, Idaho Falls, ID 83415.

coating and is most indicative of gun performance. Standard band centers for the two colors are $\lambda_{CH1} = 0.95$ μm and $\lambda_{CH2} = 1.35$ μm. Frequency response is limited to 10 Hz. The IPP is calibrated against a tungsten ribbon standard. The square of the residuals for this linear calibration is <0.995. This end-to-end calibration takes into account responsivities, area, and amplifier differences in the detectors, and when calibrated on a tungsten lamp, includes the spectral emissivity variation of tungsten.

The minimum measurable temperature of 1000 °C specified by the manufacturer is dependent on the particle material, size, and number. For materials with a spectral emissivity ratio similar to tungsten ($\varepsilon = 1.29$), the uncertainty in the absolute temperature read by the IPP is approximately ±5%. Further details of the temperature measurement technique are available in the literature (Ref 4-6).

The Mach number of the flow may be obtained from the measurements of static pressure (P_∞) and stagnation pressure (P_0). For subsonic flow, the stagnation pressure measured by the pitot tube is the true stagnation pressure (Ref 7). The freestream Mach number (M_∞) can be obtained from the direct solution of Eq 1.*

$$\frac{P_\infty}{P_0} = \left(1 + \frac{\gamma - 1}{2} M_\infty^2\right)^{-(\gamma/\gamma - 1)} \quad \text{(Eq 1)}$$

where $V_\infty = M_\infty a$

and $a = \sqrt{\gamma RT}$.

For supersonic flow, a shock wave will form in front of the probe. The total pressure measured by the probe, however, is not the freestream stagnation pressure. Rather, the stagnation pressure indicated by the pitot tube is the stagnation pressure behind a normal shock (Ref 8). The measured static pressure is a close approximation to the static pressure upstream of the shock. The upstream Mach number can be derived from the Rayleigh supersonic pitot formula (Eq 2). For P_∞/P_0 greater than 0.5283, the flow is subsonic and Eq 1 is employed, whereas for P_∞/P_0 less than 0.5283, the flow is supersonic and Eq 2 is employed.

$$\frac{P_\infty}{P_0} = \frac{\left(\frac{2\gamma}{\gamma+1} M_\infty^2 - \frac{\gamma-1}{\gamma+1}\right)^{(1/\gamma-1)}}{\left(\frac{\gamma+1}{2} M_\infty^2\right)^{(\gamma/\gamma-1)}} \quad \text{(Eq 2)}$$

3. Experimental Procedure

Spraying was performed by a Model 9000 TWEA (Tafa Inc., Concord, NH) spray system using aluminum wire with a 0.375 in. orifice (blue cap) and a short cross wire positioner. Commercially available Tafa 01T aluminum wire ($^1/_{16}$ in.) was sprayed at a voltage of 28 V. Particle size, velocity, and temperature were measured during flight for the following combination of process parameters: 100 amp/40 psi, 100 amp/60 psi, 100 amp/75 psi, 200 amp/40 psi, 200 amp/60 psi, 300 amp/40 psi, and 300 amp/60 psi.

For each case, data were taken axially along the gun centerline and at several downstream radial cross sections representative of typical standoff distances used in industry. For the above cases, downstream data were acquired at 6 mm (0.24 in.) and 76 mm (3 in.). Certain cases have additional downstream data corresponding to standoff distances of 127 mm (5 in.) and 178 mm (7 in.). The factory-standard arc shield at the torch exit was shortened to increase accessibility to the wires for this experiment. All downstream measurements are referenced to the end of the cap (Fig. 1).

4. Results and Discussion

4.1 *Relative Particle Number Density and Spray Divergence*

For the 200 amp/60 psi case, the centerline relative particle number density reaches a maximum ~22 mm downstream and quickly drops as the plume spreads out radially (Fig. 2). The relative number densities for the 100 amp and the other 200 amp

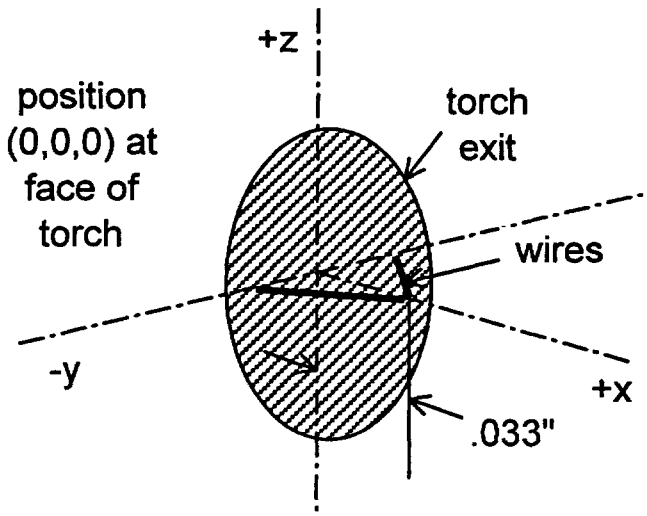

Fig. 1 Reference coordinates

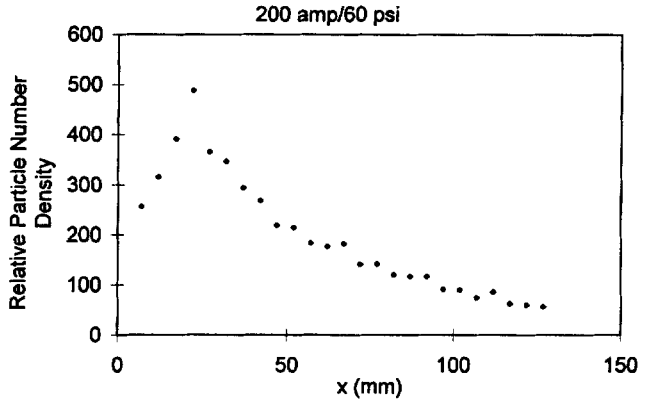

Fig. 2 Centerline particle number density, 200 amp/60 psi

*Atmospheric pressure at the 4500 ft altitude of the laboratory was 12.43 psia during these experiments, and the ratio of specific heats (γ) was set equal to 1.4.

cases peak from 16 to 22 mm downstream, whereas the 300 amp case peaks at 32 mm downstream. For any given cross section of the flow, the particle number density is the highest at the centerline of the spray and declines rapidly with distance from the centerline. Figure 3 shows the approximate shape of the spray plume and the coverage area produced by the spray gun at various standoff distances.

4.2 *Particle Size*

The drop size distribution is determined by a balance between aerodynamic shear forces, which tend to breakup the drops, and surface tension of the molten aluminum, which tends to hold the drops together (Ref 9). For all cases, the average sizes of the molten aluminum particles range from 33 to 53 μm (±2 μm). Figure 4 shows the range of average particle diameters along the spray centerline. In general, particle size decreases with decreasing current and increasing gas pressure. Average centerline particle diameters range from 33.2 to 46.0 μm for the 100 amp cases, 40.0 to 52.4 μm for the 200 amp cases, and 42.6 to 52.9 μm for the 300 amp cases. Average particle size along the spray centerline initially decreases to a minimum value at approximately 20 to 32 mm downstream, then increases slightly as the particles travel downstream. Beyond this distance, the smaller particles are flung to the outside of the spray.

One side of the spray plume had slightly larger particles, possibly due to asymmetric melting behavior of the cathode and the anode wire. Asymmetric melting behavior of the cathode and the anode wire has been captured by high speed photography and documented in the literature (Ref 10). The anode melts slowly, resulting in elongated, relatively large droplets. Some large droplets are broken up by the atomizing gas. This uneven melting leads to an asymmetry of the arc and affects the spray pattern and the coating structure. At the cathode, melting is more localized, and the molten droplets are immediately blown away by the atomizing gas flow, resulting in relatively small droplets. The higher melting rate at the cathode is thought to be due to a more constricted arc attachment compared to the more diffuse arc attachment at the anode.

Figure 5 shows the radial distribution of particle sizes at various downstream locations for the 200 amp/60 psi case. The radial scans indicate that the largest particles remain along the centerline. The average particle size decreases radially outward from the centerline. Size distributions at various cross sections for the other process parameter settings also exhibit this trend.

4.3 *Particle and Gas Velocity*

For the cases shown in Fig. 6, the peak average velocity of the particles ranges from 130 to 190 m/s (approximately ±8 m/s). This peak velocity occurs further downstream as current is increased. Higher air pressure causes a higher particle velocity at any given location in the flow since the smaller particles travel faster. Conversely, a lower gas pressure causes a larger mean particle size and lower mean particle velocity. Previous researchers have also noted this effect during the gas atomization of aluminum particles (Ref 11). The particles accelerate to a peak velocity, then they slightly decelerate as they travel downstream. This effect is especially apparent for the larger particles. The practical implication is that, for all combinations of process parameters

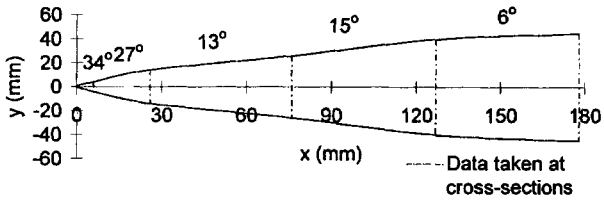

Fig. 3 Spray plume divergence

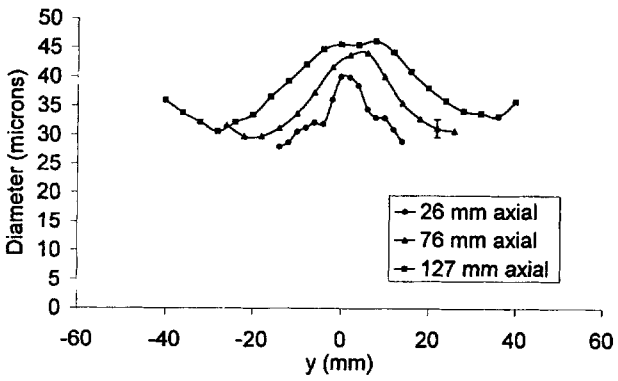

Fig. 5 Cross-sectional particle size profiles, 200 amp/60 psi

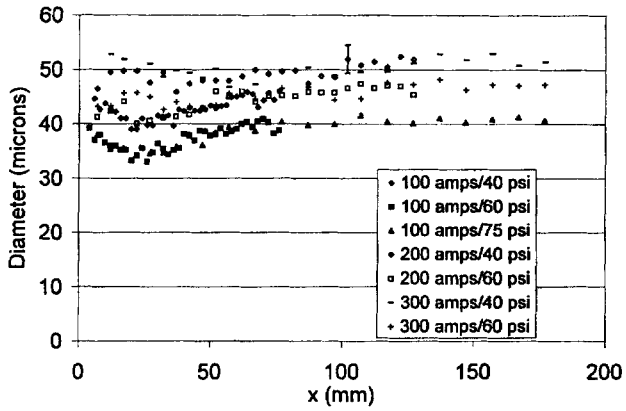

Fig. 4 Centerline average particle size

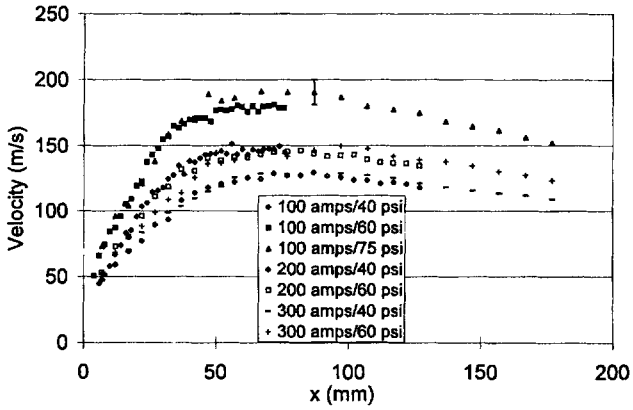

Fig. 6 Centerline average particle velocity

shown, the particle velocity at the center of the spray is essentially constant for standoff distances greater than 52 mm (2 in.).

The average particle velocity decreases at the edge of the spray due to entrainment from stagnant, ambient air. The cross-sectional velocity profiles exhibit a dip in velocity along the central region of the spray. The velocity dip is very pronounced near the wires; then it gradually flattens farther downstream. The magnitude of this dip in velocity is approximately 50 m/s for the 40 psi cases, 75 m/s for the 60 psi cases, and 100 m/s for the 75 psi case.

Data taken with a stagnation pressure probe show that this dip is due to blockage caused by the wires protruding into the flowfield. As shown in Fig. 7, the blockage effect is the greatest immediately downstream of the wires and becomes less farther downstream. A stagnation pressure probe was used to determine the effect of the wires and to qualify the velocity regime of the gas stream without the presence of particles. Both static and total pressures were measured along the centerline of the plume and at various radial cross sections to provide an indirect measurement of gas velocity.

Figure 8 shows the axial velocity of the unladen airstream (without the wires present) for a gun pressure of 75 psi and superimposes the particle velocity for the 100 amp/75 psi case. The particle velocity is evident on this plot merely for reference since it is expected that coupling between the multiphase constituents will have an effect on the air velocity. Comparison of data obtained with and without the wires present in the flowfield shows that the wires are causing a dip in velocity along the spray centerline. Figures 9(a) and (b) compare the velocity profiles of the unladen air flow 26 mm downstream with and without the wires protruding into the airstream. The flow is highly nonuniform, and the effects of blockage by the wires is evident. The stagnation pressure probe data indicate that the wires make the flow highly three-dimensional. The flow exits the gun into stagnant freestream air, causing the formation of an effective nozzle and permitting the flow to accelerate to a low supersonic velocity. Since Mach numbers greater than 0.3 exist within the flowfield, the flow can be considered compressible. Schlieren photography would be a useful tool to visualize the shock structure within the flowfield.

4.4 *Temperature Measurements*

The average centerline particle temperatures remain fairly constant as the particles travel downstream and range from 2004 to 2056 °C (approximately ±115 °C) for all seven cases (Fig. 10). The particles exhibit 1345 to 1397 °C of superheat*. The high degree of superheat indicates that the particles are fully molten upon impact at the substrate. The bright arc light inter-

*Melting point of aluminum is 659 °C.

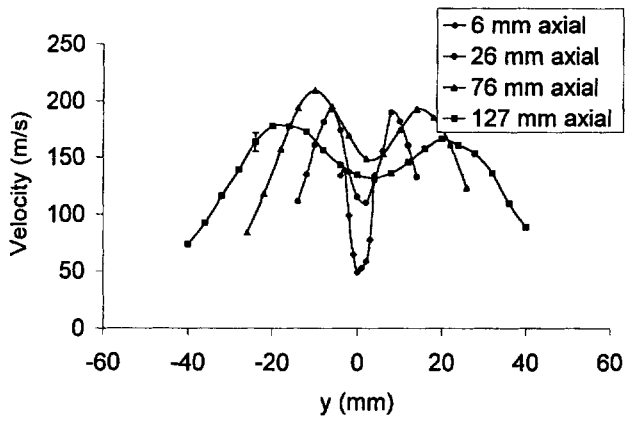

Fig. 7 Cross-sectional particle velocity profiles, 200 amp/60 psi

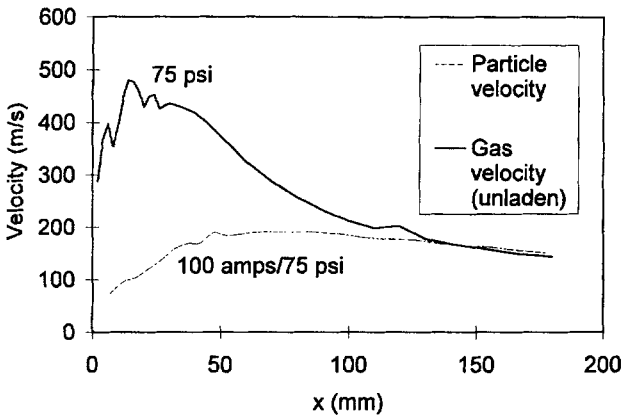

Fig. 8 Centerline air velocity for unladen flow, 75 psi

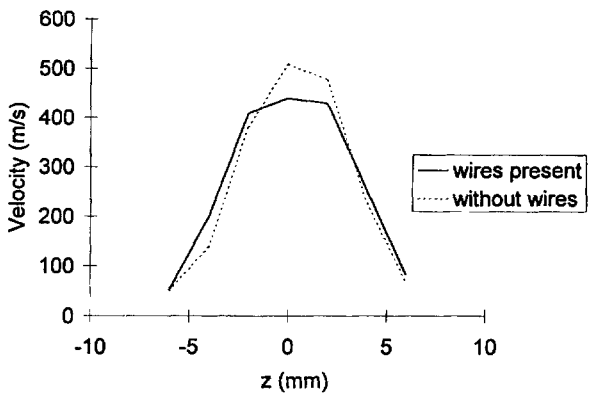

(a)

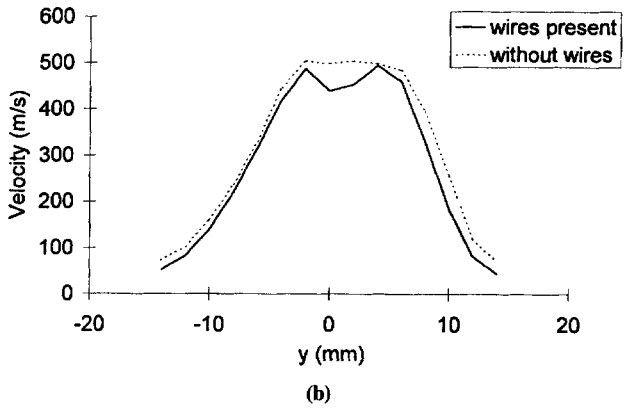

(b)

Fig. 9 (a) Unladen air velocity with and without wires present, $y = 0$, $x = 26$ mm. (b) Unladen air velocity with and without wires present, $z = 0$, $x = 26$ mm

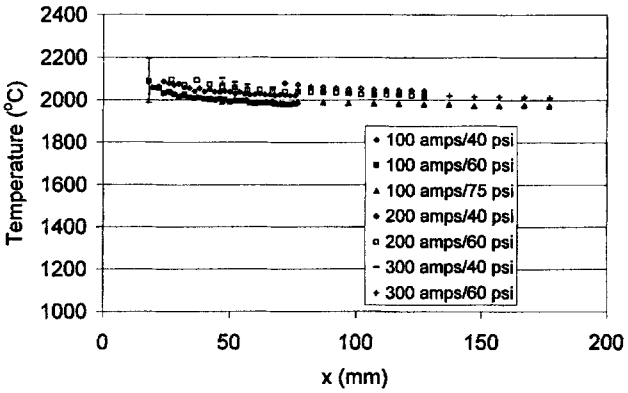

Fig. 10 Centerline average particle temperature

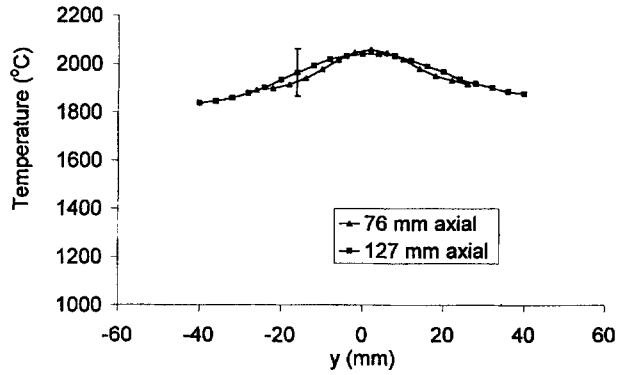

Fig. 11 Cross-sectional particle temperature profiles, 200 amp/60 psi

feres with the incandescent light measured by the IPP detectors; therefore, accurate particle temperature measurements cannot be made near the wires. The cross-sectional temperature scans show a Gaussian-type temperature profile, with the particles along the spray centerline several hundred degrees hotter than the particles at the edges of the spray. As shown in Fig. 11 for the 200 amp/60 psi case, particle temperatures are highest at the centerline and decrease by 200 °C from the centerline to the edges of the spray. This is caused by convective cooling of the particles from the entrainment of ambient air into the plume.

5. Summary

In-flight particle measurements show that there is more variation across the plume for a single case than in the downstream direction for the different process parameter settings. From the representative results presented here, the following observations are made.

5.1 *Particle Size*

- Average particle diameters along the centerline range from 33.2 to 52.9 μm for all cases in this study.
- As the particles travel downstream along the centerline of the plume, the average centerline particle sizes decrease and then increase as the flow proceeds downstream.
- The largest particles at any particular cross section are at the centerline of the spray.
- Particle size decreases with decreasing current and increasing gas pressure.
- One side of the spray plume has slightly larger particles, most likely due to larger particles coming off of the anode.

5.2 *Particle Velocity*

- Average particle velocities along the centerline peak at 130 to 190 m/s for all cases in this study.
- Cross-sectional velocity profiles reveal pronounced blockage caused by the presence of the wires in the airstream. This dip in velocity is the greatest in the particle data taken at the 26 mm downstream location. Farther downstream in the flow, the profile fills in partially, although the dip is still evident.
- The side (most likely the anode) with larger particles had slightly lower velocities. This can be attributed to asymmetric melting at the wires (Ref 10).
- Particle velocities are highest in the central region of the spray, although along the centerline there is a pronounced dip in the velocity profile. The magnitude of this dip in particle velocity is approximately 50 m/s for the 40 psi cases, 75 m/s for the 60 psi cases, and 100 m/s for the 75 psi case.
- The slowest particles are located at the edges of the spray.
- A lower gun pressure causes a larger mean particle size and lower mean particle velocity.
- The unladen air flow reaches low supersonic speeds within the flowfield. Mixed regions of subsonic and supersonic flow are present, resulting in a complex three-dimensional flowfield.

5.3 *Particle Temperature*

- Radial temperature profiles showed the hottest particles exist at the center of the spray. The shape of the temperature curve appeared nearly Gaussian. There was an approximately 200 °C temperature difference between the particles located at the centerline of the spray and those at the edges.
- Axial temperature measurements could not be taken immediately downstream of the wires due to interference from the bright arc light.
- Particle temperatures along the centerline remain fairly constant as they travel downstream. Superheat of the molten droplets ranges from 1345 to 1397 °C. For standoff distances of practical interest, the particles are fully molten upon impact at the substrate.
- Increases in current do not affect the particle temperature. At a given downstream location along the centerline, the particles produced by any of the three current settings are within 100 °C.

6. Recommendations

A technique developed for the in-flight measurement of particle size, velocity, and temperature in plasma spray fields has been successfully applied to the TWEA spray field. These data

serve to further the understanding of the TWEA spray-coating process and constitute a useful basis for the evaluation and development of modeling and computational methods.

In-flight particle data provide the necessary link between the spray process parameters and the coating characteristics. Data of this type will facilitate the development of more detailed and physically accurate models of the spray-coating process. This will result in better insight into the important process parameters and, ultimately, to better coatings.

Future experimental work should include Schlieren photography to visualize the shock structure within the flowfield. High speed photography of the droplet impacts at the substrate would provide information on the time evolution of the coating buildup.

These experiments are part of the first phase of a three-phase program. The particle data will be used as input to a multiphase thermal spray model under development. The second phase involves spraying coupons and performing metallography. The third phase involves corrosion testing of the coupons. The goal of the program is to relate the corrosion performance of the coating to the spray process parameters.

Acknowledgments

This work was supported by the Idaho National Engineering and Environmental Laboratory, managed by the Lockheed Martin Idaho Technologies Company for the U.S. Department of Energy, Idaho Operations Office under contract No. DE-AC07-94-ID13223. The aluminum wire for these experiments was donated by Tafa, Inc.

References

1. J.R. Fincke, S.C. Snyder, W.D. Swank, D.C. Haggard, and L.D. Reynolds, Diagnostic Techniques for Thermal Plasmas and Thermal Plasma Spray, Transport Phenomena in Materials Processing and Manufacturing, *The American Society of Mechanical Engineers,* book No. H00911, 1994, p 129-140
2. W.D. Swank, J.R. Fincke, and D.C. Haggard, "A Particle Temperature Sensor for Monitoring and Control of the Thermal Spray Process," *Conf. Proc. 8th National Thermal Spray,* (Houston, Texas), ASM International, Sept 1995
3. W.D. Bachalo, and M.J. House, Phase Doppler Spray Analyzer for Simultaneous Measurements of Drop Size and Velocity Distributions, *Opt. Eng.,* Vol 23 (No. 5), ASM International, 1984, p 583
4. W.D. Swank, C.H. Chang, J.R. Fincke, and D.C. Haggard, Measured and Simulated Particle Flow Field Parameters in a High Power Plasma Spray, *Proceedings of the 9th National Thermal Spray Conference* (Cincinnati, OH), Oct 1996, p 541
5. J.R. Fincke, W.D. Swank, and D.C. Haggard, Plasma Spraying of Alumina: Plasma and Particle Flow Fields, *Plasma Chem. Plasma Process.,* Vol 13, (No. 4), ASM International, Dec 1993
6. J.R. Fincke, W.D. Swank, and C.L. Jeffery, Simultaneous Measurement of Particle Size, Velocity, and Temperature in Thermal Plasmas, *IEEE Transactions on Plasma Science,* Vol 18 (No. 6), Dec 1990
7. A.H. Shapiro, *The Dynamics and Thermodynamics of Compressible Fluid Flow,* Vol 1, New York, 1953, p 83
8. J.P. Holman, *Experimental Methods for Engineers,* McGraw-Hill, Inc., 1966, p 221-222
9. G.E. McCreery, and C.M. Stoots, Drop Formation Mechanisms and Size Distributions for Spray Plate Nozzles, *Int. J. Multiphase Flow,* Vol 22 (No. 3), 1996, p 431-452
10. X. Wang, J. Heberlein, E. Pfender, and W. Gerberich, Effect of Shrouded CO_2 Gas Atomization on Coating Properties in Wire Arc Spray, *Proceedings of the 8th National Thermal Spray Conference,* (Houston, Texas), ASM International, Sept 1995
11. A.R.E. Singer, J.S. Coombs, and A.G. Leatham, The Characteristics of Aluminum Particles Produced by Gas Atomizing, *Modern Developments in Powder Metallurgy,* Vol 8, 1974, p 263-280